^{13}C NMR Relaxation Studies of Backbone and Side Chain Motion of the Catalytic Tyrosine Residue in Free and Steroid-Bound Δ^5-3-Ketosteroid Isomerase†

Qinjian Zhao,‡,§ Chitrananda Abeygunawardana,‡ and Albert S. Mildvan*,‡

Department of Biological Chemistry and Department of Pharmacology and Molecular Sciences, The Johns Hopkins University School of Medicine, Baltimore, Maryland 21205

Received October 24, 1995; Revised Manuscript Received November 30, 1995⊗

ABSTRACT: Side chain and backbone dynamics of the catalytic residue, Tyr-14, in free and steroid-bound Δ^5-3-ketosteroid isomerase (EC 5.3.3.1, homodimer, $M_r = 26.8$ kDa) have been examined by measurements of longitudinal and transverse ^{13}C relaxation rates and nuclear Overhauser effects at both 500 and 600 MHz (proton frequencies). The data, analyzed using the model-free formalism, yielded an optimized correlation time for overall molecular rotation (τ_m) of 17.9 ns, in agreement with the result (18 ns) of fluorescence anisotropy decay measurements [Wu, P., Li, Y.-K., Talalay, P., & Brand, L. (1994) *Biochemistry 33,* 7415−7422] and Stokes' law calculation (20 ns). The order parameter of the side chain C_ϵ of Tyr-14 ($S^2 = 0.74$), which is a measure of the restriction of its high-frequency (nanosecond to picosecond) motion, was significantly lower than that of the backbone C_α ($S^2 = 0.82$), indicating greater restriction of backbone motion. Upon binding of the steroid ligand, 19-nortestosterone hemisuccinate, a product analog and substrate of the reverse isomerase reaction, S^2 of the side chain C_ϵ increased from 0.74 to 0.86, while that of the backbone C_α did not change significantly. Thus, in the steroid complex, the amplitude of high-frequency side chain motion of Tyr-14 became more restricted than that of its backbone which could lower the entropy barrier to catalysis. Lower-frequency (millisecond to microsecond) motion of Tyr-14 at rates comparable to k_{cat} were detected by exchange contributions to transverse relaxation of both C_ϵ and C_α. Steroid binding produced no change in this low-frequency motion of the side chain of Tyr-14, which could contribute to substrate binding and product release, but decreased the exchange contribution to transverse relaxation of the backbone.

A quantitative description of protein dynamics is important to the mechanistic understanding of enzyme action. While many studies of protein dynamics have been made using X-ray crystallography, NMR relaxation, and theoretical calculations, little is known about the amplitude and frequency of amino acid residues directly participating in catalysis. It may be anticipated that active site residues are highly mobile in the free enzyme to permit proper substrate docking and that they become much less so in the active complex to minimize entropic barriers to catalysis. The latter concept, which has been called, among other things, freezing at reaction centers on enzymes (FARCE), has received much support from kinetic studies of model reactions of sterically and covalently restrained substrates [reviewed in Mildvan (1974)] and by direct NMR observation of enzyme-bound substrates (Nowak & Mildvan, 1972).

Aided by theoretical advances (Lipari & Szabo, 1982a,b; Palmer et al., 1991; Clore et al., 1990), heteronuclear labeling, and the development of indirect detection methods (Peng & Wagner, 1994, and references therein), NMR relaxation methods have become sensitive enough for the study of the motions of individual amino acid residues of proteins. Palmer (1993) and Wagner (1993) have reviewed these recent advances in the characterization of the internal and overall motions of small proteins by modern NMR techniques. The dynamics of several free and ligand-complexed proteins have recently been studied by ^{13}C (Nicholson et al., 1992) and ^{15}N NMR relaxation (Akke et al., 1993; Cheng et al., 1994; Rischel et al., 1994; Farrow et al., 1994; Epstein et al., 1995). A high-order parameter (S^2) reflecting localized immobilization of residues near the ligand binding site is a general observation as shown in the staphylococcal nuclease−Ca^{2+}−3′,5′pdTp complex (Nicholson et al., 1992), ion-bound calbindin D_{9k} (Akke et al., 1993), liganded FK506 binding protein (Cheng et al., 1994), acyl coenzyme A binding protein (Rischel et al., 1994), and a phosphopeptide-complexed SH2 domain (Farrow et al., 1994). Interestingly, significant decreases in order parameter were also observed in some parts of the SH2 binding domain when the ligand binds (Farrow et al., 1994). However, the dynamics of catalytic residues of enzymes, particularly in response to ligand binding, have not been reported.

The enzyme Δ^5-3-ketosteroid isomerase (EC 5.3.3.1, isomerase)[1] provides a unique opportunity for the study of the dynamics of a catalytic residue, Tyr-14. The isomerase reaction converts unconjugated Δ^5-3-ketosteroids to the cor-

† These studies were supported by NIH Grants DK 28616 (to A.S.M.) and DK 07422 (to Paul Talalay).

* Corresponding author.
‡ Department of Biological Chemistry.
§ Department of Pharmacology and Molecular Sciences.

⊗ Abstract published in *Advance ACS Abstracts,* January 15, 1996.

[1] Abbreviations: DMSO, dimethyl sulfoxide; GARP, globally optimized alternating-phase rectangular pulses; isomerase, Δ^5-3-ketosteroid isomerase (EC 5.3.3.1); MOPS, 4-morpholinepropanesulfonic acid; NMR, nuclear magnetic resonance; NOE, nuclear Overhauser effect; 19-nortestosterone, 17β-hydroxy-4-estren-3-one; 19-NTHS, 19-nortestosterone 17β-hemisuccinate; R_1, longitudinal relaxation rate constant ($1/T_1$); R_2, transverse relaxation rate constant ($1/T_2$); R_{ex}, exchange contribution to R_2; rf, radio frequency; Tris, tris(hydroxymethyl)aminomethane; TSP, 3-(trimethylsilyl)propionate-*2,2,3,3-d*$_4$.

0006-2960/96/0435-1525$12.00/0

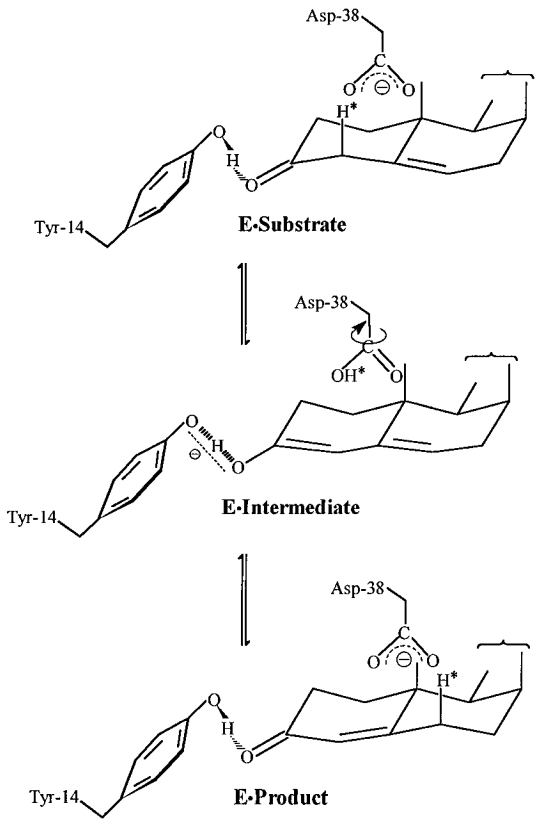

FIGURE 1: Orthogonal trans reaction mechanism of Δ^5-3-ketosteroid isomerase (Kuliopulos et al., 1991; Zhao et al., 1995a, and references therein). Tyr-14 and Asp-38 are the acid and base catalysts, respectively, in the stereospecific proton transfer from the 4β- to the 6β-position in the conversion of Δ^5-3-ketosteroids to Δ^4-3-ketosteroids. Note the orthogonal orientation of these two residues in approaching the steroid A and B rings.

responding conjugated Δ^4-3-ketosteroids utilizing Tyr-14 as a general acid and Asp-38 as a general base (Figure 1). Kinetic studies of single and double mutants have shown that the complete catalytic power of this enzyme can be explained by the concerted action of Tyr-14 and Asp-38 (Kuliopulos et al., 1989, 1990; Xue et al., 1990). The role of Tyr-14 is donation of a strong, directional hydrogen bond to the substrate in the ground state (Kuliopulos et al., 1991; Austin et al., 1992, 1995; Zhao et al., 1995a,b) and a stronger hydrogen bond to the dienolic intermediate (Xue et al., 1991; Cleland & Kreevoy, 1994), thereby rendering this intermediate thermodynamically and kinetically accessible during the isomerase reaction (Hawkinson et al., 1994). The strength of the hydrogen bond to the intermediate has been estimated to be at least 7.6 kcal/mol (Xue et al., 1991). Decreased motion of the side chain of Tyr-14 in response to the binding of a 3-ketosteroid has been detected by the selective narrowing of the UV absorption bands of this residue (Zhao et al., 1995b). Because of the qualitative nature of this observation, i.e., the difficulty in translating it into a decreased amplitude and/or frequency of motion, and because no information was provided on the backbone motion at position 14, we specifically labeled the C_α- and C_ϵ-positions of Tyr-14 in the active Y55F/Y88F mutant, in which Tyr-14 is the only tyrosine residue.[2] The k_{cat}/K_m of Y55F/Y88F is 80% of that of wild-type enzyme (Kuliopulos et al., 1991). This enabled us to use ^{13}C relaxation methods to study the amplitude and frequency of the backbone and side chain motions of Tyr-14 and the effects of steroid binding on these motions.

EXPERIMENTAL PROCEDURES

Materials. Δ^5-Androstene-3,17-dione for isomerase assays was synthesized from dehydroepiandrosterone (Kawahara et al., 1962), and 19-nortestosterone hemisuccinate (19-NTHS) from Steraloid (Wilton, NH) was purified by recrystallization from hexane/acetone. Ammonium sulfate, ampicillin, isopropyl thiopyranogalactoside, DMSO-d_6, D_2O, 4-morpholinepropanesulfonic acid (MOPS), and tricine were from Sigma (St. Louis, MO). Chelex-100 resin, reagents, and the apparatus for sodium dodecyl sulfate−polyacrylamide gel electrophoresis (SDS−PAGE) were from Bio-Rad (Richmond, CA). An L-amino acids kit from Sigma and ^{13}C(ring C_3,C_5-) and (C_α-)-labeled L-tyrosine (95−99% enrichment) from Cambridge Isotope Laboratory (Andover, MA) were used for the specific labeling of the Y55F/Y88F mutant in MOPS media. Competent cells of *Escherichia coli* strain BL21(DE3) and the expression vector pET-25b(+) were obtained from Novagen (Madison, WI). Polymin P was from Bethesda Research Lab (Gaithersburg, MD).

Expression and Purification of Specifically ^{13}C-Labeled Isomerase. E. coli BL21(DE3) transformed with the pET-25b(+) expression vector carrying the Y55F/Y88F mutant isomerase gene[3] was grown in 1 L of MOPS medium (Neidhardt et al., 1974),[4] supplemented with 2 g of glucose, 1 g of NH_4Cl, and 200 mg of each L-amino acid except tyrosine, together with 100 mg of L-tyrosine specifically labeled with ^{13}C either in the 3,5-positions of the ring (C_ϵ) or at C_α. Single colonies were used to inoculate 20 mL of LB medium containing 100 μg/mL ampicillin. When the OD_{600} (optical density) was about 1.5, the bacteria were centrifuged at 1000*g* for 5 min, resuspended in the above-mentioned MOPS media, and used to inoculate 1 L of MOPS media. Bacteria were grown at 28 °C, and isopropyl thiopyranogalactoside (1 mM) was added to induce the expression of isomerase when the OD_{600} was between 0.8 and 1.0. After 16 h of growth at 28 °C to an OD_{600} of ~2.5, the cells were harvested by centrifugation at 7000*g* for 15 min. The pellet was subjected to three cycles of freezing over dry ice and thawing in a room temperature water bath. The bacteria were then resuspended in 50 mL of 50 mM Tris-HCl (pH 7.5) buffer solution containing 100 mM NaCl, stirred over ice for 40 min, and then sonicated over ice for three periods of 10 s each. After removal of the supernatant by centrifugation at 10000*g* for 30 min, resuspension and sonication of the pellet were repeated. The supernatants were combined, and polymin P was added to a final concentration of 0.8% (w/v) to precipitate the nucleic acids. After

[2] Wild-type isomerase contains three tyrosine residues (Tyr-14, Tyr-55, and Tyr-88) among 125 amino acids per subunit. The double mutant Y55F/Y88F contains the catalytic Tyr-14 as the sole tyrosine residue in the molecule. Isomerase refers to this mutant unless stated otherwise.

[3] The gene cloning of the Y55F/Y88F mutant isomerase into the pET-25b(+) expression vector under control of the strong bacteriophage T7*lac* promoter will be reported separately.

[4] MOPS medium is a minimal medium for enterobacteria. It consists of MOPS and *N*,*N*,*N*-tris(hydroxymethyl)methylglycine (tricine) buffer (pH 7.4), containing various mineral salts and vitamins (Neihardt et al., 1974). Glucose and ammonium chloride are used as carbon and nitrogen sources, respectively. It is shown in the current study that *E. coli* grows faster and has higher final cell density in the defined MOPS medium than in the conventional M9 minimal medium.

centrifugation as above, ammonium sulfate was added to the supernatant to 85% saturation to precipitate the isomerase. The mutant isomerase was purified to electrophoretic homogeneity and crystallized according to the reported procedures (Kuliopulos et al., 1987, 1989, 1991). Purified isomerase was stored as a crystalline suspension in 30% saturated and neutralized ammonium sulfate solution at 4 °C. Routine enzyme assays were carried out with 58.0 μM Δ^5-androstene-3,17-dione in 50 mM Tris-HCl buffer (pH 7.5) in the presence of 2.0% (v/v) methanol by monitoring the absorbance increase at 248 nm (Kuliopulos et al., 1989).

Preparation of NMR Samples. NMR samples were prepared in 10 mM sodium phosphate, 20 mM sodium chloride, and 9% (v/v) DMSO-d_6, at pH 7.2 (uncorrected meter reading) in D_2O. The sodium phosphate buffer used in the preparation of NMR samples was deionized with Chelex-100 resin and filtered through a 0.22 μm filter (Millipore) before addition of DMSO-d_6. The enzyme concentration was determined on aliquots by using the absorbance at 280 nm ($\epsilon = 1890$ M^{-1} cm^{-1}) for the native enzyme at pH 7.5 and at 293 nm ($\epsilon = 2390$ M^{-1} cm^{-1}) for the ionized tyrosinate at pH 13.0. The enzyme concentrations for NMR measurements were always 0.75 mM in subunits of this dimeric enzyme. To minimize the effects of sample variation, the steroid-containing samples were derived from the steroid-free samples, after data acquisition, by addition of 4 μL of a 0.184 M solution of 19-NTHS in DMSO-d_6 to 650 μL of the enzyme solution, resulting in a steroid concentration of 1.12 mM. This water soluble Δ^4-3-ketosteroid is a product analog and a substrate of the reverse isomerase reaction (Kuliopulos et al., 1991). All NMR determinations were carried out at 27.0 °C. In prolonged NMR experiments, the enzyme retained more than 90% of its activity after 1 week at 27.0 °C.

NMR Spectroscopy. All NMR experiments were performed on Varian Unity^{plus} 600 and 500 NMR spectrometers equipped with pulsed field gradient units. The 5 mm triple resonance probes with actively shielded *z* gradients were used for T_1 and $^1H-^{13}C$ NOE experiments, and one-dimensional (1D) ^{13}C spectra were recorded with 5 mm broad band probes. The temperature calibrations (27 °C) in different spectrometers were obtained by adjusting the set temperature to produce a chemical shift difference of 4.754 ppm between the proton signals of HOD and TSP in a standard sample of TSP dissolved in ^2H_2O. ^1H and ^{13}C chemical shifts are reported relative to TSP (0.0 ppm).

A total of 24 ^{13}C relaxation rate measurements were made on four samples. In all cases, the same samples were used for measurements at both magnetic fields. The pulse schemes used to record the ^{13}C T_1 and $^1H-^{13}C$ steady-state NOE of isolated $^{13}C-^1H$ pairs in the selectively labeled protein samples are shown in panels a and b of Figure 2, respectively. These schemes are essentially simplified versions of the pulse sequences reported in Yamazaki et al. (1994) for measuring T_1 and NOE values of the C_α carbons of uniformly $^{13}C/^{15}N$-enriched proteins. Since selective-labeling schemes resulted in only single resonance proton spectra in both T_1 and NOE experiments for ^{13}C-labeled Tyr-14 at the C_ϵ- or C_α-position in isomerase, the time points for each experiment were collected as a series of ^{13}C-edited proton spectra. In the case of T_1 measurements, 10 time points corresponding to delays (*T*, Figure 2a) of 0.0, 0.3, 0.6, 0.9, ..., 2.7 s were recorded at 600 MHz and 7 time

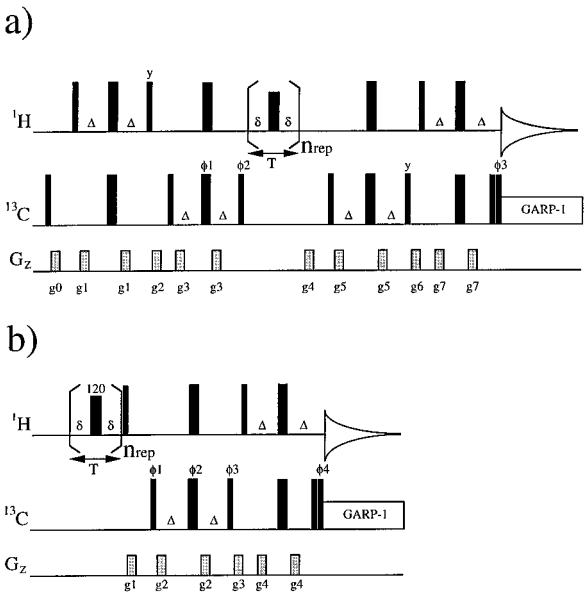

FIGURE 2: Pulse sequences for the measurements of ^{13}C R_1 (a) and steady-state ^1H ^{13}C NOE values (b) in selectively ^{13}C-labeled protein samples. Thick and thin bars correspond to 180 and 90° pulses, respectively, and unless otherwise indicated, the pulses are applied along the *x* axis. All ^1H pulses were applied with rf fields of either 36 kHz (at 600 MHz) or 25 kHz (at 500 MHz), with the exceptions of pulses during the delay *T* where a 10 kHz rf field was employed. The proton carrier was positioned at the residual HOD resonance. All carbon pulses were applied on resonance (118 or 62 ppm) with a 16 kHz rf field. GARP-1 decoupling during the acquisition time (128 ms) was with a 2 kHz field. In both experiments, the delay δ was set to 2.5 ms, requiring n_{rep} repetitions to yield the variable delay, *T*. The delay Δ was set to $1/(4^1J_{CH})$ for aromatic and aliphatic CH spin pairs which were 160 and 145 Hz, respectively. The phase cycling employed was as follows. (a) $\phi1 = (x,y,-x,-y)$; $\phi2 = 4(y),4(-y)$; $\phi3 = 8(x),8(-x)$; rec $= 2(x,-x),2(-x,x)$. (b) $\phi1 = 16(x),16(-x)$; $\phi2 = (x,y,-x,-y)$; $\phi3 = 4(y),4(-y)$; $\phi4 = 8(x),8(-x)$; rec $= 2[2(x,-x),2(-x,x)],2[2(-x,x),2(x,-x)]$. The gradients employed were as follows. (a) g0 = 0.5 ms and 5 G/cm, g1 = 0.3 ms and 3 G/cm, g2 = 1.0 ms and 8 G/cm, g3 = 0.1 ms and 5 G/cm, g4 = 0.5 ms and 10 G/cm, g5 = 0.1 ms and 4 G/cm, g6 = 0.5 ms and 5 G/cm, g7 = 0.2 ms and 4 G/cm. (b) g1 = 0.5 ms and 3 G/cm, g2 = 0.5 ms and 10 G/cm, g3 = 0.3 ms and 5 G/cm, g4 = 0.4 ms and 2 G/cm.

points corresponding to delays of 0.0, 0.3, 0.6, 0.9, ..., 1.8 s were recorded at 500 MHz. A relaxation delay of 6 s, approximately 3 times the average nonselective proton T_1, was used between scans. A total of 1024 and 2048 transients were collected for each time point in the 600 and 500 MHz T_1 data, respectively.

$^1H-^{13}C$ steady-state NOE data (Figure 2b) at both fields were recorded with and without ^1H saturation for the last 6.0 s of a 9.0 s relaxation delay. NOE experiments reached steady state with saturation periods of 5.0 s or longer. However, longer saturation times (>7.0 s) introduce some sample heating. A total of 2048 and 3072 scans were collected for each NOE spectrum at 600 and 500 MHz, respectively.

Attempts to measure R_2 by two heteronuclear methods, the Carr−Purcell−Meiboom−Gill method (Kay et al., 1989) and the $T_{1\rho}$ method (Yamazaki et al., 1994), were not successful, apparently due to very fast transverse relaxation. Hence, the ^{13}C T_2 values were extracted from the line width measurements in 1D ^{13}C spectra of the selectively labeled protein samples. Prior to the recording of these spectra, the spectrometer shims were optimized with a labeled acetate

sample (10 mM $Na^{13}CH_3COO^-$ in ^2H_2O) with identical geometry, to a line width <1 Hz at 27 °C to minimize the field inhomogeneity contribution to the line width measurements. Hence, no corrections for inhomogeneity were made to the broad resonances measured (26−55 Hz). ^{13}C spectra of protein samples were collected with a 60° flip angle, 1.0 s recycle delay, and ^1H decoupling (WALTZ-16 using 2.0 kHz on-resonance rf field) during the 1.0 s acquisition time. A total of 3200 and 8192 scans were collected for each 1D spectrum at 600 and 500 MHz, respectively.

Calculations of R_1, R_2, and NOEs. The R_1 values were calculated by plotting the peak heights (I) of the ^{13}C-edited proton signals as a function of relaxation interval (t) and fitting the data to eq 1 by a three-parameter (I_∞, I_0, and R_1) nonlinear least-squares analysis (Leatherbarrow, 1992).

$$I(t) = I_\infty - (I_\infty - I_0)\exp(-R_1 t) \tag{1}$$

In eq 1, I_0 and I_∞ are the initial and final peak heights, respectively. The transverse relaxation rates, R_2, were obtained by direct measurements of the line width (lw) at the half-height of the ^{13}C resonance peaks according to eq 2.

$$R_2 = \pi(\mathrm{lw}) \tag{2}$$

Each measured line width (26−55 Hz) was corrected for the amount of line broadening used (3−10 Hz). Within experimental error, the corrected values of R_2 were insensitive to the amount of line broadening used. Lorentzian curve fitting yielded the same R_2 values, within experimental error. Steady-state NOEs were calculated using

$$\mathrm{NOE} = I_{sat}/I_{eq} \tag{3}$$

in which I_{sat} and I_{eq} are the peak intensities in the ^{13}C-edited proton spectra recorded with and without saturation of protons during the NOE delay period, respectively. Similar NOE values, within experimental error, were obtained using peak heights or peak areas. For both R_1 and NOE measurements, minimal line broadenings were used (5 Hz or less) to minimize the contribution of natural abundance ^{13}C signals, especially in the C_α region. The R_1 and NOE values were insensitive, within experimental error, to the amount of line broadening used.

Relaxation Theory. The model-free approach characterizes both the rate and amplitude of internal motion for individual $^{13}C-H$ bond vectors using three parameters: τ_m, the isotropic tumbling time of the entire molecule, τ_e, the effective correlation time, and S^2, the order parameter (Lipari & Szabo, 1982a,b; Clore et al., 1990). S^2 is a measure of the degree of spatial restriction of the C−H vector, and its value ranges from 0, for unrestricted internal motion, to 1, for complete restriction of internal motion. Experimentally measurable relaxation parameters, R_1, R_2, and NOEs, are functions of the spectal density function, $J(\omega)$. $J(\omega)$ is a function of the above-mentioned unique motional parameters (Lipari & Szabo, 1982a,b) and is expressed as

$$J(\omega_i) = {}^2/_5\left[\frac{S^2\tau_m}{1+(\omega_i\tau_m)^2} + \frac{(1-S^2)\tau}{1+(\omega_i\tau)^2}\right] \tag{4}$$

in which

$$\frac{1}{\tau} = \frac{1}{\tau_m} + \frac{1}{\tau_e} \tag{5}$$

Since the equations cannot be solved mathematically, the approach of analyzing the relaxation data is to randomly search a whole range of these parameters to simulate the measured relaxation data. The sum of the relative errors in the calculated values of R_1, R_2, and NOEs in comparison with the experimental values can be calculated and minimized after each simulation. In some cases, a term R_{ex}, an exchange contribution to R_2, in addition to the contribution of dipole−dipole (DD) interaction and chemical shift anisotropy (CSA), is necessary to obtain satisfactory simulations as shown by eq 6.

$$R_2 = R_{2(DD)} + R_{2(CSA)} + R_{ex} \tag{6}$$

Motional parameters, τ_e, S^2, and R_{ex}, can be extracted from the optimized simulation when the analysis converges and satisfactory back calculations of the experimental values are obtained.

Simulations Using Model-Free Formalism. The spin relaxation of the ^{13}C nucleus is dominated by the dipolar interaction between the ^{13}C nucleus and the attached ^1H nucleus, as well as the chemical shift anisotropy (CSA). The CSA values of 172 ppm (Palmer et al., 1993) for the aromatic C_ϵ-carbon and 25 ppm (Spiess, 1978) for the backbone C_α-carbon of tyrosine were used in the simulations. The internuclear C−H distance of 1.09 Å was used for both the $C_\alpha-H$ and $C_\epsilon-H$ vectors in the simulations of the NOE measurements. The fits were optimized by comparison of the R_1, R_2, and NOE values calculated by Monte Carlo simulations through grid searches with the experimental data. The sum of the fractional errors in R_1, R_2, and NOEs was minimized to obtain the best fits. The use of absolute errors did not significantly alter the conclusions. The simulations and optimizations were carried out using the program Modelfree, version 3.1, kindly provided by Dr. Arthur G. Palmer, III, Columbia University (Palmer et al., 1991; Stone et al., 1993). A total of six relaxation measurements for each ^{13}C-enriched nucleus (R_1, R_2, and NOE at 500 and 600 MHz proton frequencies) were used to derive and optimize four dynamical parameters (τ_m ,τ_e, S^2, and R_{ex}).

RESULTS AND DISCUSSION

Protein Purification and Sample Preparation. The pET expression vector provided a 2-fold higher yield of soluble protein than the previously used pUC-19 vector (Kuliopulos et al., 1991). At least 40 mg of homogeneous isomerase per liter of MOPS defined medium can be obtained with the methods described in Experimental Procedures. In order to solubilize and stabilize isomerase for NMR experiments, several solvents were studied. Alkyl alcohols, frequently used in the purification of isomerase, are potent inhibitors of isomerase activity. Their potency as inhibitors increases as the alkyl chain increases (data not shown). Among all the water miscible organic solvents tested, DMSO was found to be the least potent inhibitor of isomerase under assay

conditions.[5] For this reason, DMSO was chosen as a cosolvent to study the kinetics of inhibition of isomerase and the solubility and stability of isomerase in aqueous solution. Under assay conditions (58 μM Δ^5-androstene-3,17-dione), 84% of the enzyme activity is retained in 4.5% (v/v) DMSO and 44% of the enzyme activity is retained in 9.0% (v/v) DMSO. The presence of DMSO should therefore not significantly affect the isomerase active site structure or the global conformation of this enzyme.

19-NTHS, a product analog and substrate of the reverse isomerase reaction (Kuliopulos et al., 1991), was used as the steroid ligand. Isomerase is insensitive to structural changes at the 17-position of steroids as it catalyzes the isomerization of a series of steroids with various substituents at C-17. In the presence of 9.0% (v/v) DMSO as cosolvent, 19-NTHS is a linear competitive inhibitor of the Y55F/Y88F mutant of isomerase with a K_I value of 10 $\pm$ 1 μM. Thus, in the NMR sample solution of the enzyme−steroid complex (0.75 mM isomerase plus 1.12 mM 19-NTHS), 97% of the enzyme was in the steroid-bound form.

Side Chain and Backbone Relaxation Rates of Tyr-14. Since C_α- and C_ϵ-doubly-^{13}C-labeled L-tyrosine is not available, we did specific ^{13}C labeling at C_α and C_ϵ of Tyr-14 in isomerase in two separate preparations to study the motion of the backbone and side chain in response to ligand binding. Figure 3 shows representative spectra for the determination of R_1, R_2 and NOE values. For this sizable protein (26.8 kDa), high-quality T_1 data could be obtained both for the side chain C_ϵ of Tyr-14 (Figure 4a) and for the backbone C_α-carbon (Figure 4b). The binding of the steroid ligand 19-NTHS shortens T_1 of the side chain C_ϵ of Tyr-14 and lengthens T_1 of the backbone C_α (Figure 4). Opposite effects of ligand binding on T_2 of the side chain and backbone of Tyr-14 were also observed (Table 1). For the C_ϵ-labeled Tyr-14 in isomerase, attempts to measure T_2 by the Carr−Purcell−Meiboom−Gill pulsed method were not successful as no detectable signal was seen after a total echo time of 8 ms, indicating that the T_2 values were short in the C_ϵ-labeled free enzyme. Hence, T_2 values were determined by direct ^{13}C line width measurements as described in Experimental Procedures. Table 1 summarizes the longitudinal (R_1) and transverse (R_2) relaxation rates as well as the ^{13}C NOE values of the side chain aromatic C_ϵ and backbone C_α resonances of Tyr-14. The relevant ^{13}C and ^{1}H chemical shifts are also given in Table 1.

Dynamical Parameters for High-Frequency (Nanosecond to Picosecond) Motion of Tyr-14 in Free and Liganded Isomerase. The correlation time for overall molecular rotation of ketosteroid isomerase and its complex (τ_m) was searched with the program Modelfree 3.1 initially using the ratios of the R_2 and R_1 relaxation rates measured at two ^{13}C frequencies, 125.7 and 150.9 MHz, and subsequently using the NOE measurements as well. The τ_m values for both C_α and C_ϵ agreed, wthin error, and yielded an average τ_m value of 17.9 $\pm$ 3.9 ns, which was used for all final simulations

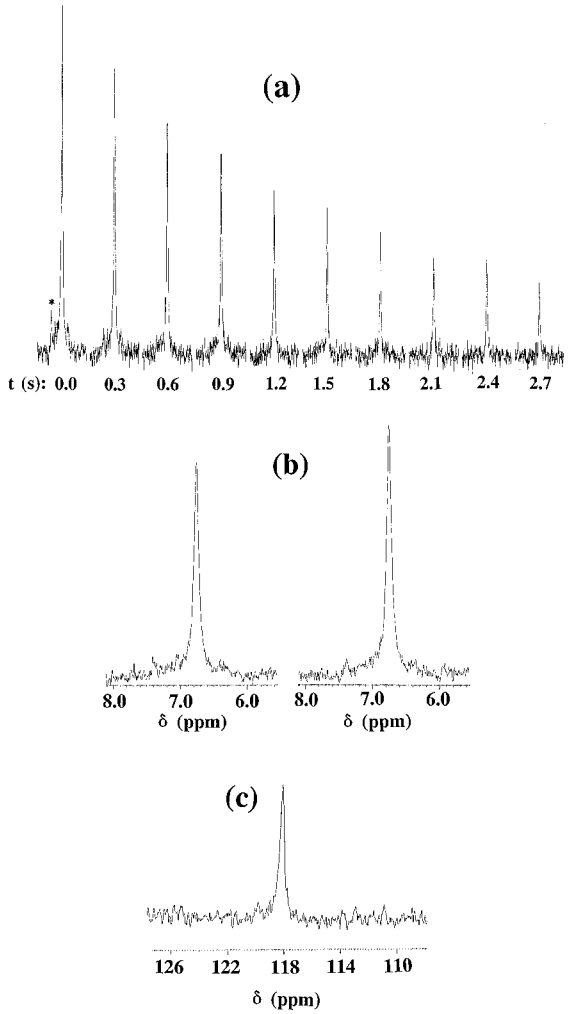

FIGURE 3: Spectra at 600 MHz (proton frequency) from the measurements of ^{13}C relaxation rates of $^{13}C_\epsilon$-labeled Tyr-14 in the 19-NTHS-liganded Y55F/Y88F mutant of isomerase. (a) $^{13}C_\epsilon$ R_1 data. The spectra were collected at 0.3 s increments in the variable delay. The asterisk (*) indicates proton signals coupled to natural abundance ^{13}C of aromatic residues of isomerase. (b) Steady-state ^{1}H−^{13}C NOE data. Spectrum of the ^{1}H-detected $^{13}C_\epsilon$ signals without (left) or with (right) ^{1}H saturation. (c) ^{13}C NMR spectrum for measurement of R_2. Line broadenings of 5 Hz were used in a and b, and 10 Hz was used in c. Other conditions are given in Experimental Procedures.

(500 each) for the free and liganded enzyme to obtain the other dynamical parameters of Tyr-14. This value of τ_m shows excellent agreement with τ_m obtained by measurements of the fluorescence anisotropy decay of the Y55F/Y88F mutant enzyme (18.0 ns, Wu et al., 1994) and the value estimated by Stokes' law calculation (20.1 $\pm$ 8.8 ns). The latter agreement indicates that the assumption of isotropic tumbling made by using eqs 4 and 5 is a valid approximation. The low-resolution X-ray crystal structure of isomerase reveals it to be a globular ellipsoid with an axial ratio of ~2.1/1 (Westbrook et al., 1984).

With this value of τ_m fixed, six measurements were used to determine three dynamical parameters in each case, the order parameter (S^2) and effective correlation time (τ_e) for high-frequency motion and the exchange contribution (R_{ex}) to transverse relaxation, resulting in well-defined values of these parameters.

The resulting model-free parameters (Table 2) indicate that the free enzyme shows a slightly greater restriction of high-

[5] Kinetic studies indicate that DMSO inhibits the enzyme as a very weak competitive inhibitor. Detailed studies of DMSO effects on the enzyme activity, stability, and inhibitor binding in the presence of DMSO will be reported elsewhere. In the free enzyme, it is unlikely that DMSO interacts specifically with Tyr-14. Even if it did, this would only make the observed effects of steroid binding on Tyr-14 relaxation appear smaller. Hence, our general conclusions on the "freezing" of Tyr-14 upon steroid binding would be unaltered.

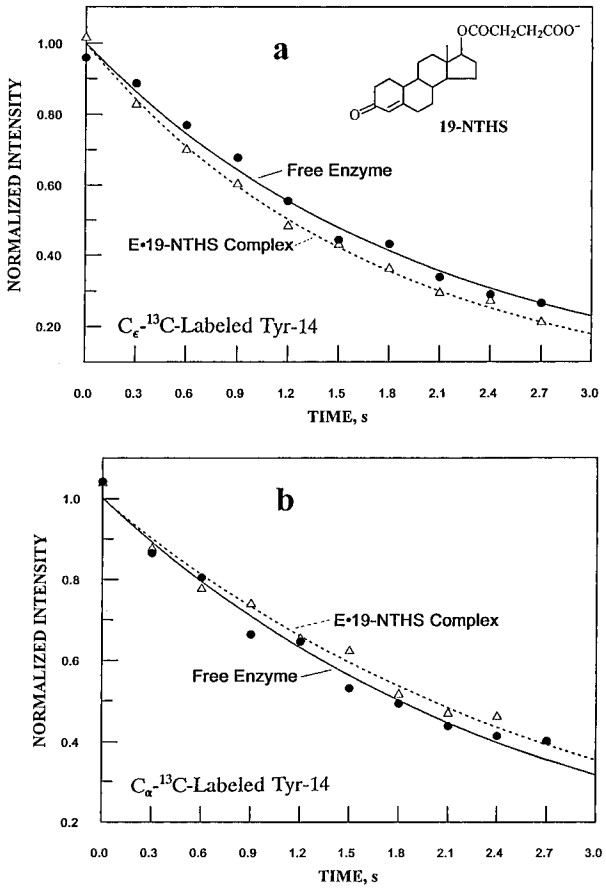

FIGURE 4: Measurements of longitudinal relaxation rates (R_1) of C_ϵ-^{13}C-labeled (a) or C_α-^{13}C-labeled (b) Tyr-14 in free (filled circles) and 19-NTHS-bound isomerase (open triangles) at 600 MHz. The theoretical curves were calculated by nonlinear least-squares fits using the program GraFit (Leatherbarrow, 1992). The structure of the inhibitor, 19-NTHS, is shown in a. Note that, for the side chain C_ϵ (a), T_1 is shorter in the complex, while for the backbone C_α (b), T_1 is slightly longer in the complex.

frequency motion of the backbone C_α than that of the side chain C_ϵ of Tyr-14, as shown by significantly different S^2 values of 0.822 and 0.741, respectively ($p = 0.015$, Table 2). The binding of the substrate analog, 19-NTHS, to isomerase significantly increases the order parameter of the side chain C_ϵ of Tyr-14 from a value of 0.741 to 0.859 ($p < 0.0001$), reflecting a decreased amplitude of motion of the side chain in the steroid complex. No change in the frequency of this motion was detected as indicated by a τ_e value of ~4.5 ps for both free and steroid-bound enzymes. This increased restriction of motion of the aromatic ring of Tyr-14 is consistent with the selective narrowing of the UV absorption bands of Tyr-14 upon steroid binding, which appears to result from the decreased amplitude of the diffusion cone and truncated modes of hydrogen bonding of the hydroxyl group of Tyr-14 (Zhao et al., 1995b).

In contrast with its effects on the side chain motion of Tyr-14, steroid binding does not further restrict the backbone motion of this residue as indicated by the small and statistically insignificant decrease in the order parameter of C_α ($p = 0.076$, Table 2). Thus, in the steroid complex, the amplitude of high-frequency side chain motion of Tyr-14 ($S^2 = 0.859$) becomes more restricted than that of its backbone ($S^2 = 0.766$) ($p = 0.0004$, Table 2). Using the simple model of diffusion in a cone, steroid binding decreases the cone semiangle of the side chain of Tyr-14 from 25 to 18°, a value significantly lower than that of the backbone (24°, Table 2). In this model, a cone semiangle of 90° indicates completely unrestricted motion ($S^2 = 0$), and an angle of 0° indicates totally restricted motion ($S^2 = 1$) (Table 2, Figure 5). Hence, as a result of steroid binding, Tyr-14, a catalytic residue which donates a hydrogen bond to the 3-keto group of 19-NTHS (Figure 5; Kuliopulos et al., 1991; Austin et al., 1992, 1995; Zhao et al., 1995a,b), becomes more restricted in the amplitude of its side chain motion than in its backbone motion in the complex. Such restriction of high-frequency motion may facilitate the attainment of the transition state for the enzyme-bound substrate by lowering the entropy barrier (Mildvan, 1974). A similar observation was recently made by ^{15}N relaxation in the binary dihydrofolate reductase−folate complex in which two tryptophan residues (Trp-22 and Trp-30) in the active site show greater S^2 values for the side chain indole N−H vectors than for the respective backbone amide ^{15}N−H vectors (Epstein et al., 1995).

Dynamical Parameters for Low-Frequency (Millisecond to Microsecond) Motion of Tyr-14 in Free and Liganded Isomerase. In all cases, for both the side chain C_ϵ and backbone C_α of free and liganded isomerase, it was necessary to include exchange contributions (R_{ex}) to the transverse relaxation rates to obtain satisfactory back calculations of the measured relaxation rates of Table 1. The sizeable R_{ex} contributions (Table 2) indicate that a reversible change in the chemical environment of Tyr-14, both in the free enzyme and in the steroid complex, is required to simulate the data. The magnitude of R_{ex} is a function of the exchange rate constant (k_{ex}), the chemical shift difference, and the population in the two environments (Epstein et al., 1995, and references therein). This change in the chemical environment of Tyr-14 could well result from exchange between two conformers of this residue and/or by aromatic ring flipping. The rate constant (k_{ex}) for such an exchange process is in the range 10^3-10^6 s^{-1} (Epstein et al., 1995, and references therein). It is of interest that the rate of the enzyme-catalyzed reaction, which is limited by the rate of substrate enolization (Xue et al., 1990, 1991), has a k_{cat} value of 1.2×10^4 s^{-1} which is in the range of the k_{ex} values. As shown in Table 2, the binding of 19-NTHS does not alter the R_{ex} contribution to R_2 of the side chain of Tyr-14 but decreases the R_{ex} contribution to R_2 of its backbone.[6] Thus, the low-frequency motion of the side chain of Tyr-14, which is unaffected by the ligand, is kinetically competent to be a part of the catalytic process. Since this low-frequency motion occurs in the free enzyme, it cannot be caused by exchange between free and steroid-bound enzyme, a process which is $\geq 10^5$ s^{-1} (Xue et al., 1990). However, this motion, which may include aromatic ring flipping, could facilitate the rapid binding and dissociation of steroids. This observation is similar to the finding with triosephosphate isomerase by solid state deuterium NMR that the motion of a loop near the active site, which is also on the time scale of its k_{cat} (5×10^3 s^{-1}), is unaffected by ligand binding (Williams & McDermott, 1995).

[6] The reason for the decrease in the R_{ex} contribution at C_α upon steroid binding is not clear. In principle, it could result from an increased inequality of populations, an increased exchange rate, or a decreased chemical shift difference between two (or more) environments for the backbone C_α of Tyr-14.

Table 1: Chemical Shifts, Relaxation Rates, and NOEs from NMR Measurements Using Proton-Detected ^{13}C NMR Spectroscopy with Specifically C_ϵ-^{13}C-Labeled or C_α-^{13}C-Labeled Tyr-14 in Free and 19-NTHS-Bound Isomerase (Y55F/Y88F Mutant, M_r = 26.8 kDa) at 27.0 °C

	C_ϵ-^{13}C-labeled Tyr-14 in isomerase		C_α-^{13}C-labeled Tyr-14 in isomerase	
	free enzyme	E·19-NTHS	free enzyme	E·19-NTHS
chemical shifts (ppm)[a]				
^1H	6.67[b]	6.75[b]	3.92[c]	3.92
^{13}C	118.45	118.20	62.00[c]	62.00
relaxation parameters at 125.71 MHz[d]				
R_1 (s^{-1})	0.716 ± 0.024	0.774 ± 0.019	0.563 ± 0.030	0.539 ± 0.013
	(0.666 ± 0.016)	(0.755 ± 0.011)	(0.551 ± 0.020)	(0.499 ± 0.010)
R_2 (s^{-1})	109 ± 5	119 ± 6	104 ± 5	66 ± 3
	(108 ± 3)	(119 ± 3)	(107 ± 3)	(74 ± 2)
NOE	1.20 ± 0.03	1.14 ± 0.03	1.41 ± 0.08	1.18 ± 0.07
	(1.18 ± 0.01)	(1.15 ± 0.01)	(1.22 ± 0.02)	(1.16 ± 0.01)
relaxation parameters at 150.86 MHz[d]				
R_1 (s^{-1})	0.492 ± 0.020	0.575 ± 0.011	0.384 ± 0.020	0.337 ± 0.017
	(0.523 ± 0.013)	(0.588 ± 0.008)	(0.390 ± 0.014)	(0.349 ± 0.010)
R_2 (s^{-1})	130 ± 7	141 ± 7	129 ± 6	91 ± 4
	(130 ± 5)	(142 ± 5)	(126 ± 4)	(80 ± 3)
NOE	1.20 ± 0.03	1.16 ± 0.03	1.15 ± 0.07	1.15 ± 0.07
	(1.19 ± 0.02)	(1.15 ± 0.02)	(1.24 ± 0.02)	(1.17 ± 0.02)

[a] Proton and carbon chemical shifts were referenced from TSP under the same conditions. [b] The downfield shift (0.08 ppm) of the ring 3,5-protons induced by 19-NTHS binding is consistent with the previous observations using the same mutant with all phenylalanines deuterated in the aromatic ring (Kuliopulos et al., 1991). [c] The significant upfield shift (−0.51 ppm) of the C_α-proton from the value of Tyr in random coils (4.43 ppm, Wishart et al., 1991) and downfield shift (6.4 or 3.9 ppm) of the C_α-carbon resonance from the average value of Tyr in random coils (55.6, Wishart et al., 1991; 58.1 ppm, Spera & Bax, 1991) indicate that Tyr-14 is in an α-helix (Wishart et al., 1991). This observation is consistent with the conclusion from a low-resolution X-ray crystallographic study of wild-type isomerase that residues 8−17 form an α-helix (Kuliopulos et al., 1987, and references therein). [d] The standard deviations of R_1 were from the nonlinear least-square fits, and those for R_2 and NOEs were derived from the signal-to-noise ratios of the spectra. The numbers in parentheses are relaxation rates ± one standard deviation back-calculated from the optimized motional parameters given in Table 2.

Table 2: Order Parameters (S^2), Effective Correlation Times (τ_e), and Exchange Contributions (R_{ex}) from Monte Carlo Simulations of the Relaxation Parameters of C_ϵ-^{13}C-Labeled or C_α-^{13}C-Labeled Tyr-14 in Free and 19-NTHS-Bound Isomerase[a]

	C_ϵ-^{13}C-labeled Tyr-14 in isomerase		C_α-^{13}C-labeled Tyr-14 in isomerase	
	free enzyme	E·19-NTHS	free enzyme	E·19-NTHS
	dynamics parameters from Monte Carlo simulations using model-free formalism[b]			
S^2 [c]	0.741 ± 0.020	0.859 ± 0.016	0.822 ± 0.032	0.766 ± 0.023
τ_e (ps)	4.4 ± 0.9	4.5 ± 2.2	5.0 ± 1.4	0.7 ± 0.6
R_{ex} (s^{-1})[d]	41 ± 6	39 ± 5	62 ± 5	21 ± 3
	semiangle of the cone using the simple diffusion model[e]			
θ (deg)	25	18	21	24

[a] Results from 500 Monte Carlo simulations using the program Modelfree Version 3.1 written by A. G. Palmer, III (Columbia University, 1995), to minimize the sum of the relative errors in R_1, R_2, and NOE (Palmer et al., 1991). The uncertainties in the parameters are the standard deviations from the simulations. [b] Assuming liganded enzyme and free enzyme have the same rotational correlation time, an average τ_m value of 17.9 ± 3.9 ns was obtained from estimations using R_2/R_1 ratios and optimizations using subsets of the relaxation data. This value is consistent with 18.0 ns determined by time-resolved fluorescence measurements (Wu et al., 1994) and estimation using Stokes' law (20 ns). Thus, τ_m = 17.9 ns was fixed for the final simulations to obtain the other dynamics parameters. [c] S^2 (0−1), the order parameter, measures the restricted amplitude of motion of the ^{13}C−H vector. Statistical tests (Dunn, 1977) of the significance of the differences in S^2 yielded the following p values: C_ϵ in free versus liganded enzyme, $p < 0.0001$; C_α in free versus liganded enzyme, $p = 0.076$; C_α versus C_ϵ in free enzyme, $p = 0.015$; and C_α versus C_ϵ in liganded enzyme, $p = 0.0004$. [d] R_{ex} values are given at 600 MHz. The values at 500 MHz are lower by the factor $(500/600)^2$. [e] Order parameter (S^2) correlates with the semiangle (θ) of the "wobbling in a cone" model, according to the following equation (Lipari & Szabo, 1982b), $S^2 = [\cos\theta\,(1 + \cos\theta)/2]^2$.

CONCLUSION

It is shown from ^{13}C relaxation measurements and model free simulations of the dynamics of Tyr-14 that the global rotation of isomerase occurs with a time constant of 18 ns in agreement with that found by fluorescence anisotropy decay and Stokes' law calculations. When high-frequency (nanosecond to picosecond) internal motions of Tyr-14 are studied, the side chain of this catalytic residue shows higher amplitude motion than the backbone. Upon steroid binding, the side chain becomes more immobilized ("frozen"), whereas the amplitude of motion of its backbone is unaltered. As a result, in the steroid complex, the side chain motion of Tyr-14 has become more restricted than the backbone motion. When low-frequency (millisecond to microsecond) motions, comparable to the rate of catalysis, are studied, ligand binding produced no change in the side chain motion of Tyr-14 but decreased the exchange contribution of its backbone. Hence, the concept of freezing at reaction centers on enzymes (FARCE) applies only to high-frequency side chain motions in this case. The biological significance of the decreased amplitude of high-frequency motion of the side chain of Tyr-14 upon steroid binding is that such freezing may facilitate the attainment of the transition state for the enzyme-bound substrate by lowering the entropy barrier. The low-frequency side chain motions, unaltered by steroid binding, may reflect processes such as aromatic ring flipping which could facilitate the rapid binding and dissociation of substrates and products.

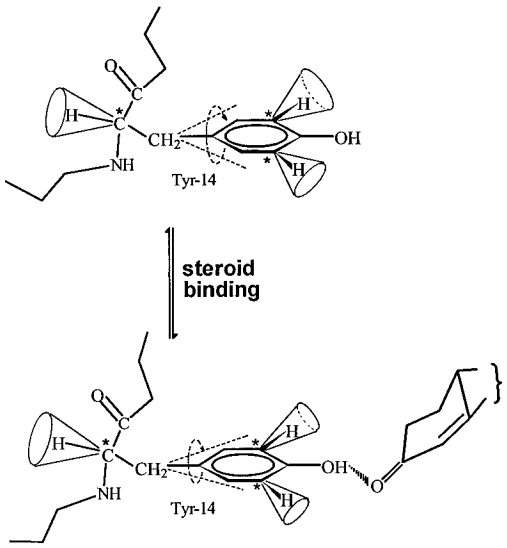

FIGURE 5: Amplitudes of high-frequency motions of the C_α−H and both side chain C_ϵ−H vectors of Tyr-14 of isomerase and response to steroid binding based on the "wobbling in a cone" model using the cone semiangles in Table 2. Wobbling of the two degenerate C_ϵ−H vectors of Tyr-14 implies restricted motion of the entire aromatic ring as a unit, which is in accord with the narrowing of UV absorption bands (π to π^*) of Tyr-14 induced by ligand binding (Zhao et al., 1995b). The decrease in amplitude of side chain motion of Tyr-14 upon steroid binding is statistically significant, but the increase in amplitude of backbone motion is not. Asterisks (*) indicate the positions of ^{13}C labeling of tyrosine.

ACKNOWLEDGMENT

We thank Dr. Paul Talalay for his advice and helpful comments, Dr. Arthur G. Palmer, III, for providing the program Modelfree (Version 3.1) and for valuable discussions, Dr. Lewis E. Kay for providing the pulse sequences for uniformly ^{15}N- or ^{13}C-labeled proteins which we modified and used in this work, and Gale Doremus for help in preparation of the manuscript.

REFERENCES

Akke, M., Skelton, N. J., Palmer, A. G., III, & Chazin, W. J. (1993) *Biochemistry 32*, 9832−9844.
Austin, J. C., Kuliopulos, A., Mildvan, A. S., & Spiro, T. G. (1992) *Protein Sci. 1*, 259−270.
Austin, J. C., Zhao, Q., Jordan, T., Talalay, P., Mildvan, A. S., & Spiro, T. G. (1995) *Biochemistry 34*, 4441−4447.
Cheng, J.-W., Lepre, C. A., & Moore, J. M. (1994) *Biochemistry 33*, 4093−4100.
Cleland, W. W., & Kreevoy, M. M. (1994) *Science 264*, 1887−1890.
Clore, G. M., Szabo, A., Bax, A., Kay, L. E., Driscoll, P. C., & Gronenborn, A. M. (1990) *J. Am. Chem. Soc. 112*, 4989−4991.
Dunn, O. J. (1977) *Basic Statistics: A Primer for the Biomedical Sciences*, 2nd ed., pp 65−70, John Wiley & Sons, New York.
Epstein, D. M., Benkovic, S. J., & Wright, P. E. (1995) *Biochemistry 34*, 11037−11048.
Farrow, N. A., Muhandiram, R., Singer, A. U., Pascal, S. M., Kay, C. M., Gish, G., Shoelson, S. E., Pawson, T., Forman-Kay, J. D., & Kay, L. E. (1994) *Biochemistry 33*, 5984−6003.
Hawkinson, D. C., Pollack, R. M., & Ambulos, N. P., Jr. (1994) *Biochemistry 33*, 12172−12183.
Kawahara, F. S., Wang, S.-F., & Talalay, P. (1962) *J. Biol. Chem. 237*, 1500−1506.
Kay, L. E., Torchia, A., & Bax, A. (1989) *Biochemistry 28*, 8972−8979.
Kuliopulos, A., Shortle, D., & Talalay, P. (1987a) *Proc. Natl. Acad. Sci. U.S.A. 84*, 8893−8897.
Kuliopulos, A., Westbrook, E. M., Talalay, P., & Mildvan, A. S. (1987b) *Biochemistry 26*, 3927−3937.
Kuliopulos, A., Mildvan, A. S., Shortle, D., & Talalay, P. (1989) *Biochemistry 28*, 149−159.
Kuliopulos, A., Mullen, G. P., Xue, L., & Mildvan, A. S. (1991) *Biochemistry 30*, 3169−3178.
Leatherbarrow, R. J. (1992) *GraFit* Version 3.0, Erithacus Software Ltd., Staines, U.K.
Lipari, G., & Szabo, A. (1982a) *J. Am. Chem. Soc. 104*, 4546−4559.
Lipari, G., & Szabo, A. (1982b) *J. Am. Chem. Soc. 104*, 4559−4570.
Mildvan, A. S. (1974) *Annu. Rev. Biochem. 43*, 357−399.
Neidhardt, F. C., Bloch, P. L., & Smith, D. F. (1974) *J. Bacteriol. 119*, 736−747.
Nicholson, L. K., Kay, L. E., Baldisseri, D. M., Arango, J., Young, P. E., Bax, A., & Torchia, D. A. (1992) *Biochemistry 31*, 5253−5263.
Nowak, T., & Mildvan, A. S. (1972) *Biochemistry 11*, 2813−2818.
Palmer, A. G., III. (1993) *Curr. Opin. Biotechnol. 4*, 385−391.
Palmer, A. G., III, Rance, M., & Wright, P. E. (1991) *J. Am. Chem. Soc. 113*, 4371−4380.
Palmer, A. G., III, Hochstrasser, R. A., Millar, D. P., Rance, M., & Wright, P. E. (1993) *J. Am. Chem. Soc. 115*, 6333−6345.
Peng, J. W., & Wagner, G. (1994) *Methods Enzymol. 239*, 563−596.
Rischel, C., Madsen, J. C., Andersen, K. V., & Poulsen, F. M. (1994) *Biochemistry 33*, 13997−14002.
Spera, S., & Bax, A. (1991) *J. Am. Chem. Soc. 113*, 5490−5492.
Spiess, H. W. (1978) *NMR: Basic Princ. Prog. 15*, 55.
Stone, M. J., Chandrasekhar, K., Holmgren, A., Wright, P. E., & Dyson, H. J. (1993) *Biochemistry 32*, 426−435.
Wagner, G. (1993) *Curr. Opin. Struct. Biol. 3*, 748−754.
Westbrook, E. M., Piro, O. E., & Sigler, P. B. (1984) *J. Biol. Chem. 259*, 9096−9103.
Williams, J. C., & McDermott, A. E. (1995) *Biochemistry 34*, 8309−8319.
Wishart, D. S., Sykes, B. D., & Richards, F. M. (1991) *J. Mol. Biol. 222*, 311−333.
Wu, P., Li, Y.-K., Talalay, P., & Brand, L. (1994) *Biochemistry 33*, 7415−7422.
Xue, L., Talalay, P., & Mildvan, A. S. (1990) *Biochemistry 29*, 7491−7500.
Xue, L., Talalay, P., & Mildvan, A. S. (1991) *Biochemistry 30*, 10858−10865.
Yamazaki, Y., Muhandiram, R., & Kay, L. E. (1994) *J. Am. Chem. Soc. 116*, 8266−8278.
Zhao, Q., Mildvan, A. S., & Talalay, P. (1995a) *Biochemistry 34*, 426−434.
Zhao, Q., Li, Y.-K., Mildvan, A. S., & Talalay, P. (1995b) *Biochemistry 34*, 6562−6572.

BI9525381